

Complex polymer topologies in blends: Shear and elongational rheology of linear/pom-pom polystyrene blends

V. Hirschberg, S. Lyu and M. G. Schußmann

Citation: *Journal of Rheology* **67**, 403 (2023); doi: 10.1122/8.0000544

View online: <https://doi.org/10.1122/8.0000544>

View Table of Contents: <https://sor.scitation.org/toc/jor/67/2>

Published by the [The Society of Rheology](#)

ARTICLES YOU MAY BE INTERESTED IN

[Dilute polymer solutions under shear flow: Comprehensive qualitative analysis using a bead-spring chain model with a FENE-Fraenkel spring](#)

Journal of Rheology **67**, 373 (2023); <https://doi.org/10.1122/8.0000517>

[On the nature of flow curve and categorization of thixotropic yield stress materials](#)

Journal of Rheology **67**, 461 (2023); <https://doi.org/10.1122/8.0000558>

[Confined Brownian suspensions: Equilibrium diffusion, thermodynamics, and rheology](#)

Journal of Rheology **67**, 433 (2023); <https://doi.org/10.1122/8.0000520>

[Viscous dissipation in large amplitude oscillatory shear of unsaturated wet granular matter](#)

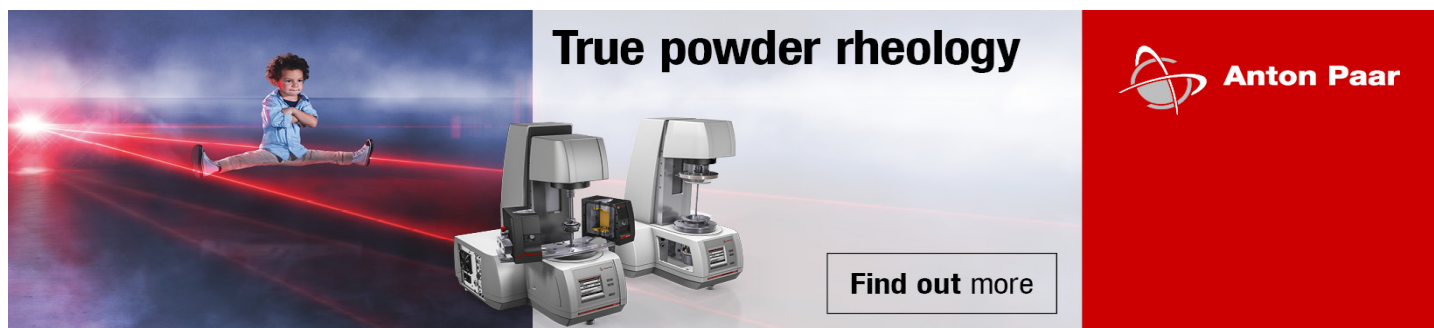
Journal of Rheology **67**, 365 (2023); <https://doi.org/10.1122/8.0000507>

[Determination of the molecular weight distribution of ultrahigh molecular weight polyethylene from solution rheology](#)

Journal of Rheology **66**, 1079 (2022); <https://doi.org/10.1122/8.0000502>

[Improving stretchability of associative polymers through tuning density of the secondary interactions^{a\)}](#)

Journal of Rheology **67**, 293 (2023); <https://doi.org/10.1122/8.0000508>



The advertisement features a composite image. On the left, a young child in a blue shirt and shorts is performing a handstand on a dark surface, with red laser lines extending from their feet across the floor. In the center, two Anton Paar rheometers are shown. The text 'True powder rheology' is prominently displayed in the upper right. The Anton Paar logo and name are in the bottom right corner. A 'Find out more' button is located at the bottom center.

True powder rheology

Anton Paar

Find out more



Complex polymer topologies in blends: Shear and elongational rheology of linear/pom-pom polystyrene blends

V. Hirschberg,^{a)} S. Lyu, and M. G. Schußmann

Institute for Chemical Technology and Polymer Chemistry, Karlsruhe Institute of Technology (KIT), Engesserstraße 18, Karlsruhe 76131, Germany

(Received 5 August 2022; final revision received 20 December 2022; published 13 January 2023)

Abstract

The shear and elongational rheology of linear and pom-pom shaped polystyrene (PS) blends was investigated experimentally and modeled using constitutive models such as the Doi–Edwards and the molecular stress function (MSF) model. The pom-pom molecule is the simplest topology to combine shear thinning with strain hardening in elongational flow. A PS pom-pom with a self-entangled backbone ($M_{w,bb} = 280 \text{ kg mol}^{-1}$) and 22 entangled sidearms ($M_{w,a} = 22 \text{ kg mol}^{-1}$) at each star was blended with two linear PS with weight average molecular weights of $M_w = 43$ and 90 kg mol^{-1} and low polydispersities ($\mathcal{D} < 1.05$). A semilogarithmic relationship between the weight content of the pom-pom, $\phi_{\text{pom-pom}}$, and the zero-shear viscosity was found. Whereas the pure pom-pom has in uniaxial elongational flow at $T = 160 \text{ }^\circ\text{C}$ strain hardening factors (SHFs) of $\text{SHF} \approx 100$, similar values can be found in blends with up to $\phi_{\text{pom-pom}} = 50 \text{ wt. } \%$ in linear PS43k and PS90k. By blending only 2 wt. % pom-pom with linear PS43k, $\text{SHF} = 10$ can still be observed. Furthermore, above $\phi_{\text{pom-pom}} = 5\text{--}10 \text{ wt. } \%$, the uniaxial extensional behavior can be well-described with the MSF model with a single parameter set for each linear PS matrix. The results show that the relationship between shear and elongational melt behavior, i.e., zero-shear viscosity and SHF, can be uncoupled and customized tuned by blending linear and pom-pom shaped polymers and very straightforwardly predicted theoretically. This underlines also the possible application of well-designed branched polymers as additives in recycling. © 2023 Author(s). All article content, except where otherwise noted, is licensed under a Creative Commons Attribution (CC BY) license (<http://creativecommons.org/licenses/by/4.0/>). <https://doi.org/10.1122/8.0000544>

I. INTRODUCTION

Blends of polymers are of high interest and are often used in industrial processes because of the tunability of the desired processing properties as well as for the final application. Due to their industrial relevance, the shear and elongational melt behavior of blends based on many polymers with a linear and branched topology needs to be investigated in the linear [1,2] and the nonlinear regime [3,4] and for time-dependent excitations. For example, the blends of linear low-density polyethylene (LLDPE) with low-density polyethylene (LDPE) [5–7], linear and branched polypropylene (PP) [8–10], different grades of poly(lactic acid) (PLA) [11] or polystyrene (PS) with styrene-butadiene-styrene (SBS) rubbers [12] were studied. Model PS blends, e.g., those containing two linear chains [13–16] or a mixture of linear chains and rings [17,18], have been the focus of many studies due to their unique properties under elongational flow, allowing the validation of constitutive models and molecular theories, such as the (extended) interchain pressure model [19]. Linear polymers show in elongational flow rather weak strain hardening at strain rates above the inverse of the Rouse relaxation time, but no strain hardening can be observed below it [1]. However, higher processing temperatures are very beneficial for processing due to lower

viscosities, so strain hardening at high temperatures is extremely desirable. It is commonly known that strain hardening can be induced by long chain branching [20–24] or by blending small amounts of ultrahigh molecular weight (UHMW) compounds with lower MW grades [25–27]. Blending with UHMW components has the disadvantage of an increased zero-shear viscosity η_0 . For example, the blend of a linear PS with $M_w = 430 \text{ kg mol}^{-1}$ and $\eta_0 = 7.97 \times 10^5 \text{ Pa s}$ at $T = 160 \text{ }^\circ\text{C}$ with only 1.5 wt. % of an UHMW PS with $M_w = 15.000 \text{ kg mol}^{-1}$ results in a near doubling of η_0 to $1.39 \times 10^6 \text{ Pa s}$, whereas the strain hardening factors (SHFs) increase from nearly none to the range of 5–7 [27]. Following the idea of the tube model, strain hardening is created on the molecular level by chain stretching [28]. At strain rates below the inverse of the Rouse time, τ_R , chain stretching can be induced by chain branching, because of the stretching of the segments between two branching points. Consequently, at least two branching points within the molecule are required to create strain hardening [29]; thus, the simplest topology that fulfills this requirement is the pom-pom topology, or the H-shaped molecule with an arm number $q = 2$ at each end of the backbone [30]. In general, the pom-pom topology combines two properties that are very favorable for processing: (1) thinning under shear deformation and (2) strain hardening in elongational flow [23,29,31]. Experimentally, high SHF above 10 are observed for branched structures with at least two branching points, such as comb [20,23,32,33], pom-pom [34], or Cayley-tree [35] topologies.

^{a)} Author to whom correspondence should be addressed: valerian.hirschberg@kit.edu

Following the pom-pom hypothesis, strain hardening of a pom-pom molecule originates from the stretch of the backbone [29,36] so that longer backbones should be correlated with more strain hardening. In our previous work, we observed for two pom-pom molecules with backbone molecular weight, $M_{w,bb}$, of 100 and 280 kg mol⁻¹, arm molecular weight, $M_{w,a}$, of 22 kg mol⁻¹ and an arm number of $q=22$, that the SHF increased with the backbone from 19 to 141, i.e., about a factor seven increase in SHF. From a processing point of view, a disadvantage of a longer backbone of a pom-pom molecule is a higher zero-shear viscosity. However, this seems favorable for strain hardening. The zero-shear viscosity is determined by the molecular parameters of the branched structure itself, resulting for a longer backbone in higher zero-shear viscosities. Recent research investigated the blends of linear and ring PS, showing a huge impact of the blending and the possibility to create and tune nonlinear extensional properties due to threading of the ring molecules by linear chains [18], although both topologies are not branched. This can be explained by the formation of a physical quasibranching by the threaded rings along the polymer chains.

Blends of commercial PE are often investigated, due to their high industrial/commercial relevance. For example, blends of LDPE and LLDPE consist of branched and mainly linear PE chains, respectively. For one system of LDPE/LLDPE blends in elongational extension, a similar maximal SHF of about SHF = 10 was found for the pure LDPE as well as for up to 80 wt. % LLDPE [37]. At very low Hencky strain rates, $\dot{\epsilon}$, of less than 0.1 s⁻¹, partly higher SHF of up to 20 were observed for the LDPE/LLDPE blends as for the pure LDPE between 40 and 80 wt. % LLDPE. This is attributed to phase separation between LDPE and LLDPE but might be also a temperature-driven artifact since the measurements were performed at 130 °C, and at higher temperatures phase separation should disappear. Furthermore, Wagner *et al.* found that, for the blends with up to 90 wt. % LLDPE, the molecular stress function (MSF) model with the model parameters β and f_{max}^2 for the pure LDPE and the linear spectrum of the respective blend can very well describe the elongational behavior for Hencky strain rates above 0.1 s⁻¹.

The tube model [38,39] forms the basis for the Doi-Edwards (DE) model [40]. The DE model predicts the behavior of linear polymers in both shear and elongation. The DE time-dependent stress tensor $\sigma(t)$ is given by

$$\sigma(t) = \int_{-\infty}^t m(t-t') S_{DE}^{IA}(t, t') dt', \quad (1)$$

where $m(t-t')$ is the memory function, defined as $m(t-t') = dG(t-t')/dt'$ with $G(t)$ as the relaxation modulus [41]. The orientation tensor $S_{DE}^{IA}(t, t')$ is expressed by an integral over a unit vector sphere, reading

$$S_{DE}^{IA}(t, t') = 5 \left\langle \frac{u'u'}{u'^2} \right\rangle_0, \quad (2)$$

with the unit vector u' . The symbol $\langle \dots \rangle_0$ is an average

integral over a unit vector sphere and is expressed by Eq. (3) [42],

$$\langle \dots \rangle_0 = \frac{1}{4\pi} \oint [\dots] \sin\theta_0 d\theta_0 d\varphi_0. \quad (3)$$

The DE model assumes that the diameter a_0 of the constraining tube of the model polymer chain is unaffected during the deformation and the polymer chain remains in its equilibrium state [40,43,44]. However, strain hardening is assumed to originate from the stretching of the backbone segments so that the DE model underestimates strain hardening of branched polymer chains in elongational flow. An approach to describe strain hardening behavior and to incorporate chain stretching into the DE model is the MSF model, assuming the tube diameter to decrease during elongational flow [43,44]. The change in tube diameter is included into the DE stress tensor via the MSF $f(t, t')$,

$$\sigma(t) = \int_{-\infty}^t m(t-t') f^2(t, t') S_{DE}^{IA}(t, t') dt'. \quad (4)$$

The MSF $f(t, t')$ is the inverse of the relative tube diameter, i.e., the initial tube diameter a_0 over that of time t , $a(t, t')$,

$$f(t, t') = \frac{a_0}{a(t, t')}. \quad (5)$$

The MSF $f(t, t')$ can be derived from the energy balance equation, assuming that f^2 is proportional to the stored strain energy in the system [44,45],

$$\frac{df^2}{dt} = \dot{\epsilon} \frac{\beta f^2}{1 + \frac{\beta - 1}{f^4}} \left(S_{11} - S_{22} - \frac{(f^2 - 1)}{(f_{max}^2 - 1)} \sqrt{S_{11} + \frac{1}{2} S_{22}} \right). \quad (6)$$

The two fitting parameters are β and f_{max} . It is assumed that there are β segments in the tube, of which one is the backbone, stretched in the flow direction and $(\beta - 1)$ are side chains, which are compressed [44]. Consequently, β relates to the ratio of segments in the whole polymer relative to the segments stretched, representing the slope of the strain hardening. For a linear chain, β equals one and higher values of β represent a higher number of branches [46]. The maximum possible stretching is represented by f_{max} , relating to the elongational viscosity.

Driven by a synthetic route based on anionic polymerization techniques that offer full control over molecular parameters, at a maximum degree of their variability [34], we synthesized defined pom-pom chains [47,48] and studied the impact of topology on the rheological properties. The objective of this article is to investigate the effect of blending a pom-pom shaped PS with linear monodisperse PS on the shear rheological behavior, in particular, the zero-shear viscosity, and the strain hardening behavior in elongational flow. With the synthetic route here presented, it is possible to

synthesize 10–50 g of pom-pom material within typically 10 days in our laboratory. Here, a PS pom-pom model system with a self-entangled backbone ($M_{w,bb} = 280 \text{ kg mol}^{-1}$) and $q = 22$ entangled sidearms ($M_{w,a} = 22 \text{ kg mol}^{-1}$) at each end of the backbone has been synthesized. This pom-pom shows exceptional SHFs >100 at a temperature of $160 \text{ }^\circ\text{C}$, which is significantly above SHF described in the literature for pom-poms [49], and with exception for comb [20,23,50] and barbwire type structures [51]. The high SHF allows us to clearly distinguish and quantify the effect of blending with linear PS. Two linear PS, PS43k and PS90k, with $M_w = 43$ and 90 kg mol^{-1} are used and blended with the pom-pom as $\phi_{\text{pom-pom}} = 75, 50, 20, 10, 5, 2,$ and $1 \text{ wt. } \%$ pom-pom. Observing SHF up to SHF = 4 and 10 for blends of PS43k with only 1 and 2 wt. % pom-pom compared to no strain hardening for the linear PS underlines the potential of polymers with a pom-pom topology as a polymeric additive in processing and especially toward recycling, to incorporate and tune a high SHF into the materials.

II. MATERIALS AND EXPERIMENTAL SETUP

The linear PS was synthesized by living anionic polymerization [52,53], and the pom-pom shaped PS by a combination of sequential living anionic polymerization and grafting onto as shown schematically in Fig. 1 [34]. Here, PS anions are grafted onto a polyisoprene-*b*-polystyrene-*b*-polyisoprene (ISI) triblock copolymer, where the PI blocks are functionalized via epoxidation. A more detailed explanation on this synthesis route can be found in [54–56] and in earlier work of us [34].

The linear PS have $M_w = 43 \text{ kg mol}^{-1}$ and a dispersity of $\bar{D} = 1.04$ as well as $M_w = 90 \text{ kg mol}^{-1}$ and $\bar{D} = 1.05$, respectively. The blends were made by a four step solvent blending procedure similar to the one described in the literature [57]. First, linear and pom-pom PS were both dissolved in tetrahydrofuran (THF) at room temperature and stirred overnight, followed by slow evaporation and final drying under vacuum for 24 h at $40 \text{ }^\circ\text{C}$ and a final 2h drying at $115 \text{ }^\circ\text{C}$, slightly above the glass transition temperature (T_g) of PS to remove last remaining traces of THF. An overview of the pom-pom, the linear PS, the blends and their weight contents, and their rheological properties is given in Table I.

The oscillatory shear and uniaxial extensional rheology was conducted on an ARES-G2 rheometer (TA Instruments, Newcastle, USA) using a 13 mm plate-plate geometry for the

shear measurements as well as an extensional viscosity fixture (EVF) for uniaxial elongational tests. Samples were hot-pressed at $180 \text{ }^\circ\text{C}$ for 10 min under vacuum. Shear rheology is measured between 130 and $220 \text{ }^\circ\text{C}$, using a frequency range of $\omega = 0.1\text{--}100 \text{ rad s}^{-1}$. The elongational tests were performed at $160 \text{ }^\circ\text{C}$, between Hencky strain rates of $\dot{\epsilon} = 0.03$ and to 10 s^{-1} , with maximum Hencky strains of $\epsilon = 4$, where the measurement conditions are below the inverse Rouse relaxation time of both linear PS of $\tau_R = \tau_c Z^2$ with $\tau_c = 0.005 \text{ s}$ and $M_{c,PS} = 15 \text{ kg/mol}$, yielding for PS43k 0.045 s and for PS90k 0.18 s . Considering the pom-pom as a comb, τ_R can be estimated by $\tau_R = \tau_c Z_{BB} (Z_{BB} + qZ_a)$, resulting in $\tau_R = 9.7 \text{ s}$. Consequently, i.e., strain hardening should occur at Hencky strain rates above 22.2 and 5.5 s^{-1} for PS43k and PS90k and above 0.1 s^{-1} for the pom-pom. The constitutive models, such as the DE model and the MSF model [44], were calculated using the IRIS software from Winter and Mours [58,59], by first loading the elongational data as well as the G' and G'' mastercurves of the melts into the software and calculating the Maxwell modes. In the second step, the model parameters β and f_{max}^2 are adjusted so that the MSF model predicts well and describes the highest strain hardening behavior, with β adjusting the slope and f_{max}^2 to the maximum tensile stress growth coefficient reached.

III. SHEAR RHEOLOGY

To determine the impact of blending pom-pom shaped and linear PS, first shear rheology was measured. Figure 2 shows the storage G' and loss G'' modulus mastercurve as a function of the angular frequency $a_1\omega$ of the pure pom-pom and the linear PS43k and PS90k. The pom-pom molecule exhibits a two-step relaxation process: the sidearms relax at high frequencies and the backbone at lower ones, before the complete molecule is relaxed and the terminal regime is reached, with $G' \propto \omega^2$ and $G'' \propto \omega^1$. The two clearly distinct rubber plateaus observed indicate entanglement of sidechain and backbone, so the molecule fulfills the requirements of the “pom-pom hypothesis” to be considered as not only a topological but also a rheological pom-pom regarding the definition of the pom-pom model [29]. From the comparison with the two linear PS, it can be seen that the relaxation of the sidearms of the pom-pom is significantly slower than that of the linear PS43k and as it would have been expected from their molecular weight. Similar trends were reported in the

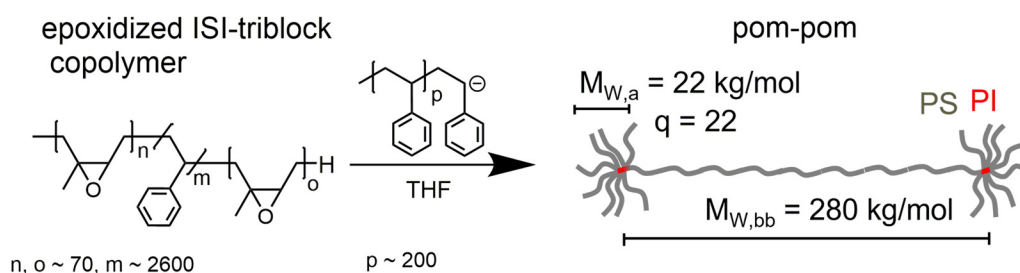


FIG. 1. Synthesis of the pom-pom PS by a combination of anionic polymerization and grafting onto: living PS anions are grafted on an ISI triblock copolymer, where the PI blocks are functionalized via epoxidation, yielding a pom-pom shaped molecule, with full control over all molecular parameters and allowing high arm numbers.

TABLE I. Overview table of the polymers and blends used, the pom-pom content $\phi_{\text{pom-pom}}$ in the blends, the total molecular weight, $M_{w,t}$, their zero-shear viscosity and the maximum SHF obtained for the specific material.

Sample	$\phi_{\text{pom-pom}}$	$M_{w,t}$ (kg mol^{-1})	η_0 (Pa s)	SHF _{max}
PS43k	0	43	3000	
1 wt. % PS43k	1		3060	4
2 wt. % PS43k	2		3620	10
5 wt. % PS43k	5		3950	15
10 wt. % PS43k	10		6100	33
20 wt. % PS43k	20		12 450	65
50 wt. % PS43k	50		46 200	121
75 wt. % PS43k	75		231 500	105
PS90k	0	90	25 000	
1 wt. % PS90k	1		26 900	1.5
2 wt. % PS90k	2		27 200	4
5 wt. % PS90k	5		36 500	8
10 wt. % PS90k	10		52 650	15
20 wt. % PS90k	20		55 000	33
50 wt. % PS90k	50		120 800	89
75 wt. % PS90k	75		250 400	84
Pom-pom280k-2x22-22k	100	1248	965 000	134

literature for highly branched PS combs with self-entangled backbones [20,60].

The $|\eta^*|$ of the pure pom-pom and blends with PS43k and PS90k is shown in Figs. 3(a) and 3(b), respectively, as a function of the frequency, or rather $a_T\omega$. Compared with a linear PS with the same total molecular weight, the zero-shear viscosity of the pom-pom is about a factor of 200 lower. The mastercurves of the blends investigated and the corresponding shift factors can be found in the supplementary material [72]. The zero-shear viscosity of PS43k ($\eta_0 = 3000$ Pa s) and PS90k ($\eta_0 = 24\,700$ Pa s) differs by about a factor of 10, so differences between their blends can be quantified clearly. A blend of a pom-pom and a linear PS exhibits a three-step relaxation process, so in every frequency regime there is a dominating relaxation process. Comparing,

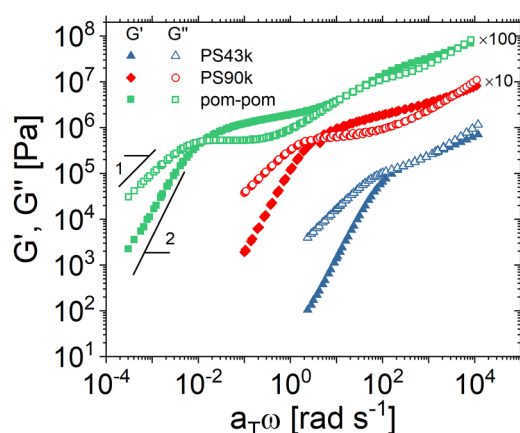


FIG. 2. Storage G' and loss G'' mastercurve of the pure PS pom-pom280k-2x22-22k, revealing a self-entangled backbone, which fulfills the requirements of the pom-pom hypothesis, as well as of PS43k and PS90k, at a reference temperature $T_{\text{ref}} = 160$ °C.

e.g., $\phi_{\text{pom-pom}} = 20$ and 2 wt. % in Fig. 3(a) or $\phi_{\text{pom-pom}} = 50$ and 2 wt. % in Fig. 3(b), higher pom-pom contents result in specific frequency regimes in lower $|\eta^*|$, although a higher pom-pom content results in higher η_0 . This difference around 10 rad s^{-1} must result from the dilution effect after the relaxation of the arms, as also seen in Fig. 5. Similar findings were currently reported for a H-shaped polymer diluted in linear PS [61]. Furthermore, at pom-pom contents below $\phi_{\text{pom-pom}} = 20$ wt. %, $|\eta^*|$ only reaches a plateau at very low frequencies after a long regime with a slight slope.

In Figs. 3(a) and 3(b), the zero-shear viscosity visibly decreases with increasing linear PS content and is shown in Fig. 3(c) as a function of the weight content of the pom-pom in the linear PS matrix. The zero-shear viscosity depends on the pom-pom content via a semilogarithmic relationship, i.e., on the amount of branched polymer between the two limits of the zero-shear viscosity of the linear PS and the pom-pom, determining the slope of the dependency. A similar semilogarithmic correlation between the zero-shear viscosity and the blend fractions was found in the literature for, e.g., blends of HDPE and LDPE [62] as well as for linear/3-arm star poly(hydroxybutyrate) blends with 18.5 and 15.8 entanglements in the arm of the star and the linear chains, respectively [63].

To further investigate the effect of blending linear and pom-pom shaped PS, the van Gurp–Palmen (vGP) plot—the phase angle δ as a function of the complex modulus $|G^*|$ —is investigated. The vGP plot allows one to investigate the impact of polymer topology on the viscoelastic properties, in a first approximation independent of their molecular weight. In Fig. 4, the vGP plot is shown in (a) for the blends with PS43k and in (b) with PS90k. The δ minimum at $|G^*| = 2 \cdot 10^5$ Pa originates from the linear PS chains as well as the arms of the pom-pom280k-2x22-22k. For the blends with PS43k and PS90k, the minimum caused by the backbone of the pom-pom280k-2x22-22k is shifted to lower $|G^*|$ and higher δ values before it vanishes completely for PS43k at $\phi_{\text{pom-pom}} = 2$ wt. % and for PS90k at $\phi_{\text{pom-pom}} = 5$ wt. %. Consequently, below those threshold values, the presence of pom-pom in the linear PS is hardly detectable in shear measurements, matching the viscosity curves in Figs. 3(a) and 3(b).

To investigate the relaxation behavior of the diluted pom-pom, G' is shown in Fig. 5 as a function the frequency for the pure pom-pom, the linear PS43k and PS90k, in (a) and (b), respectively, and of their corresponding 50 wt. % blends. For the blend with PS43k in Fig. 5(a), it can be seen that after the relaxation of the linear chains G' of the 50 wt. % blend decreases rapidly, and the backbone relaxation is highly accelerated by about a factor of 15. Similarly, the blend with PS90k in (b) shows a drastic speed up of the relaxation process of the backbone, which is, however, less significant than for the blend with PS43k. Similar trends were observed for 10 wt. % of a H-shaped polymer blended in linear PS with different MW or for star/linear blends [63,64]. Furthermore, it also shows a G' decrease around $1\text{--}10 \text{ rad s}^{-1}$ below the G' values from the PS90k, originating from the arm relaxation of the pom-pom. For the PS43k blend, this effect is not observed due to an overlap of the

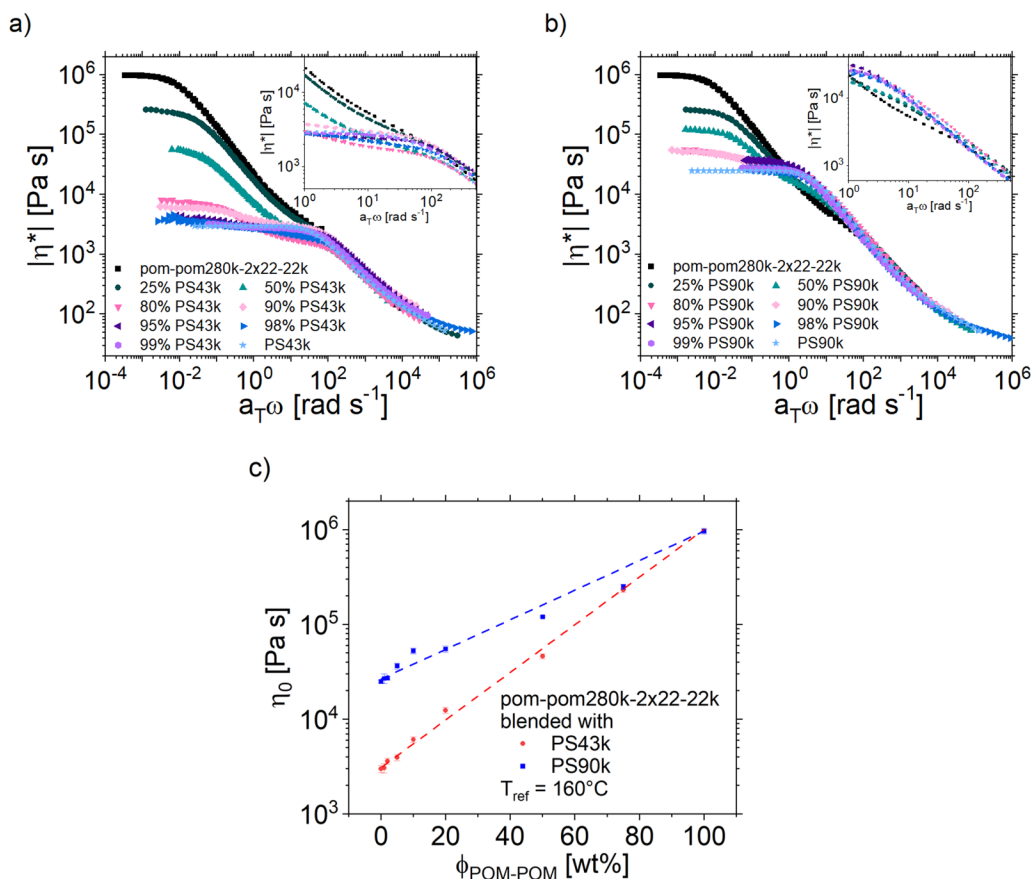


FIG. 3. The complex viscosity as a function of $a_T\omega$ for the blends with (a) PS43k and (b) PS90k as well as (c) the zero-shear viscosity as a function of the pom-pom content at a reference temperature of 160 °C, revealing a semilogarithmic correlation between zero-shear viscosity and pom-pom content.

arm relaxation with the relaxation of the linear PS43k. Additionally, this highlights a difference between regular H-shaped polymers and pom-pom used here. Due to the high number of 22 sidechains on every side of the pom-pom, the 50 wt. % blends contain 38 wt. % arms. After they are relaxed, their volume fraction is apparently high enough to enable them to act as a solvent for not only the backbone, but also for the linear chains so that G' is in this frequency regime $G'(\omega)$ lower.

To further analyze the dilution effect of the linear chains and the sidechains on the backbone, the diluted modulus $G_{N,S}^0$, which is determined as the G' value at the low frequency $\tan(\delta)$ minimum, is plotted in Fig. 6 as a function of the pom-pom backbone volume fraction. The diluted modulus $G_{N,S}^0$ is in the range of $\phi_{BB} = 0.1-1$ proportional to ϕ_{BB}^2 , $G_{N,S}^0 \sim \phi_{BB}^2$, for the linear PS as well as the pure pom-pom and the PS43k and PS90k blends with 75 and 50 wt. % pom-pom, where the backbone is self-entangled.

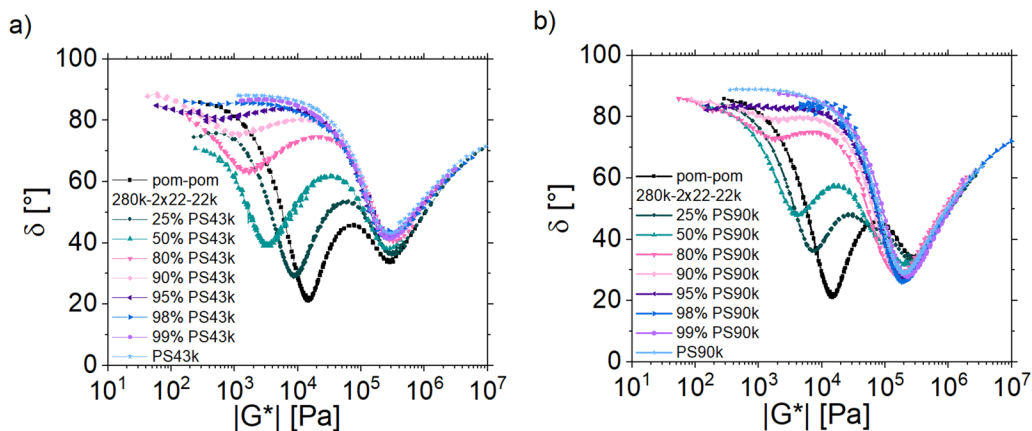


FIG. 4. vGP plot of the blends with (a) PS43k and (b) PS90k. Two distinct minima can be seen, relating at high frequencies to the relaxation of the arms and the linear chains and at low frequencies to the relaxation of the pom-pom backbone.

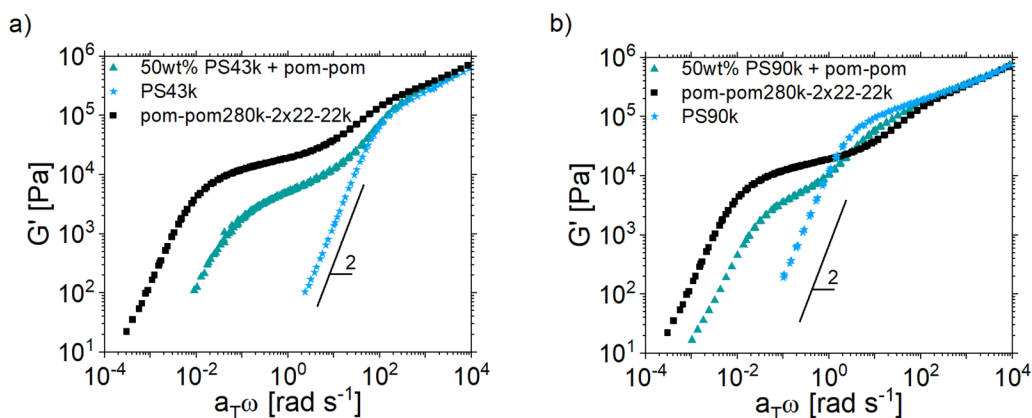


FIG. 5. G' as a function of $a_T\omega$ for the pure pom-pom, the linear PS43k and PS90k as well as of their 50 wt. % blends in (a) and (b), respectively. The pom-pom backbone relaxes in the blend earlier, clearly showing the dilution effect of the linear PS on the relaxation behavior of the pom-pom backbone.

This is in agreement with the dilution theory, predicting $G_{N,s}^0 \sim \phi_{BB}^{(1+\alpha)}$ with $\alpha = 1$ or $4/3$, i.e., in this case with $\alpha = 1$. Between $\phi_{BB} = 0.1$ and 1, for the pom-pom and the pom-pom/linear blends with self-entangled backbone, $G_{N,s}^0$ as a function of ϕ_{BB} also overlaps with other model systems reported in the literature, e.g., combs [20] or a pom-pom [34]. For a pom-pom [49] and comb blends [60] reported in the literature, it was not possible to extract $G_{N,s}^0$ precisely, but could be estimated from their mastercurves. For the pom-pom ($\phi_{BB} = 50\%$, $G_{N,s}^0 \approx 50\,000$ Pa), the pure comb ($\phi_{BB} = 38\%$, $G_{N,s}^0 \approx 25\,000$ Pa) and a 50 wt. % blend with linear PS ($\phi_{BB} = 19\%$, $G_{N,s}^0 \approx 4\,000$ Pa), where the backbones are self-entangled, $G_{N,s}^0$ is within the $G_{N,s}^0 \sim \phi_{BB}^2$ trend of the here presented experimental data. For the blends with unentangled backbones due to the dilution with the linear chains, it was found as expected $G_{N,s}^0 \sim \phi_{BB}^1$, so that $\alpha = 0$.

IV. ELONGATIONAL RHEOLOGY

To investigate the impact of pom-pom shaped molecules as melt processing additive, the extensional rheological behavior was investigated. Figures 7 and 8 show the tensile

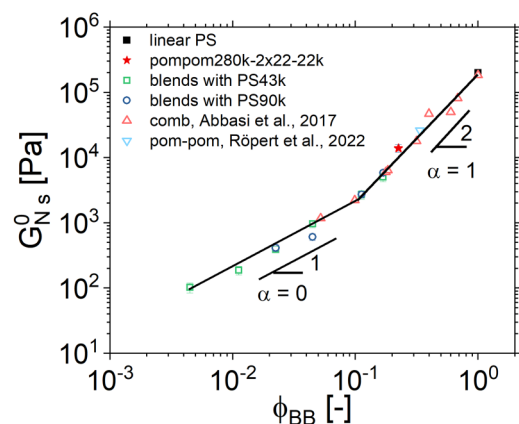


FIG. 6. The dilution modulus, $G_{N,s}^0$, as a function of the volume fraction of the backbone, ϕ_{BB} for the investigated pom-pom/linear blend systems. Additionally, data for comb [20] and pom-pom model systems [34] are added from the literature. Above $\phi_{BB} = 0.1$, when the backbone of the pom-pom is self-entangled, a slope of 2 is found and for $\phi_{BB} < 0.1$ the slope is 1.

stress growth coefficient, η_E^+ , as a function of the step time, t , for the blends with PS43k and PS90k investigated at $T = 160^\circ\text{C}$ in the range from $\dot{\epsilon} = 0.03$ to 10 s^{-1} . The full lines represent the modeling with the MSF model, the dashed lines represent the DE model. For the MSF model, one set of parameters β and f_{max}^2 is used per blend so that the highest strain hardening is predicted correctly. The linear viscoelastic (LVE) envelopes are marked as the full blue line and are calculated via the Trouton ratio from the complex viscosity from the shear mastercurve. Thus, the plateau value at long experimental step times decreases with increasing linear PS content, similar to η_0 . At low pom-pom contents of $\phi_{\text{pom-pom}} < 20\text{ wt. \%}$, the relaxation process of the linear PS dominates, so the LVE envelope has in an intermediate regime between 0.1 and 10 s a slight slope before reaching a plateau value, e.g., for the blends with $\phi_{\text{pom-pom}} = 1\text{--}10\text{ wt. \%}$ presented in Figs. 7(e)–7(h) and 8(e)–8(h). Figures 7 and 8 reveal that, at medium to high strain rates, the blends show strain hardening behavior, independent of the pom-pom content. At low Hencky strain rates, no strain hardening could be observed and measured. Evidently, strain hardening is most pronounced for the blends with 75 and 50 wt. % pom-pom but can still be observed even at only $\phi_{\text{pom-pom}} = 1\text{ wt. \%}$. Under the measurement conditions, no strain hardening can be observed for pure PS90k and PS43k. At Hencky strains above four, some polymers like LDPE [65,66] were found to show an overshoot of the tensile stress growth coefficient at Hencky strains larger than four, before reaching the elongational viscosity. Due to experimental limitations, we could not reach those Hencky strains; thus, it remains an open question to investigate with the adequate equipment.

Furthermore, it can be seen quantitatively that strain hardening is more pronounced for the PS43k blends than for the PS90k blends at a similar pom-pom weight content; however, $\eta_{E,max}^+$ is higher for the blends with PS90k than with PS43k.

The experimental data in Figs. 7 and 8 can be modeled with the MSF model using $\beta = 3$, where only the second model parameter f_{max}^2 needs to be adjusted to describe the experimental data accurately. The model parameter β controls the slope of the tensile stress growth coefficient during strain hardening, whereas f_{max}^2 relates to its steady state value, i.e.,

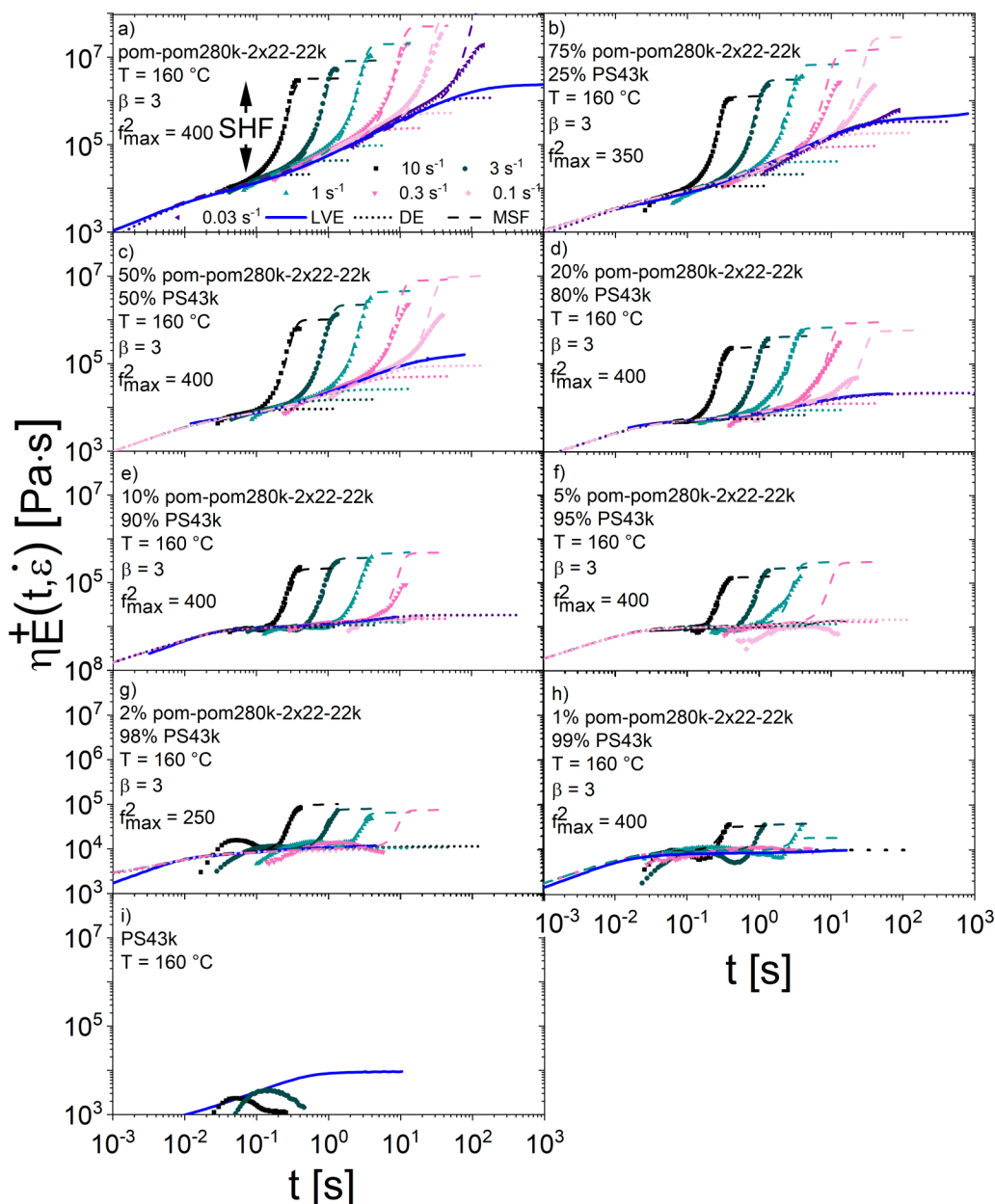


FIG. 7. The tensile stress growth coefficient as a function of the step time for pom-pom280k-2x22-22k and the blends of linear PS43k with the pom-pom for $\phi_{\text{pom-pom}} = 100, 75, 50, 20, 10, 5, 2, 1,$ and 0 wt. % pom-pom at a temperature of $T = 160$ °C.

the elongational viscosity. It needs to be mentioned that f_{max}^2 is chosen so that the maximum strain hardening is described properly. This resulted especially for the blends with PS90k in a systematic overestimation of the elongational viscosity at high Hencky strain rates. An overestimation at low Hencky strain rates might be due to a complex relaxation spectrum of the Maxwell modes, which do not only decay for some of the blends, but rather show a shoulder at intermediate relaxation times. Figure 9 shows f_{max}^2 as a function of the pom-pom content. The pure pom-pom has $f_{\text{max}}^2 = 400$. For the blends of PS43k and the pom-pom, above $\phi_{\text{pom-pom}} = 5$ wt. % little influence from the pom-pom content on $f_{\text{max}}^2 = 400$ is observed, i.e., the MSF model parameters of $\beta = 3$ and $f_{\text{max}}^2 = 400$ are not changed and can well describe the elongational behavior. For the PS90k blends, from $\phi_{\text{pom-pom}} = 10$ wt. % on, the MSF model with $\beta = 3$ and $f_{\text{max}}^2 = 300$ predicts well

the experimentally observed behavior. Similar results have been reported for LDPE/LLDPE blends [37,60], where, e.g., $\beta = 1.6$ and $f_{\text{max}}^2 = 60$ describe the elongational behavior well for blends of up to 80% LLDPE at 125 °C [60].

To quantify the effect of strain hardening behavior, the SHF is calculated and shown in Fig. 10(a) for the blends with PS43k and in (b) with PS90k. The SHF is calculated as the ratio of the maximum tensile stress growth coefficient and the predicted tensile stress growth coefficient by the DE model. The pure pom-pom has a very high SHF above 100 for $\dot{\epsilon} > 1$ s $^{-1}$ with the maximum SHF of $\text{SHF}_{\text{max}} = 134$ at $\dot{\epsilon} = 10$ s $^{-1}$.

For the blends with PS43k, the highest SHF can be observed at medium to large Hencky strain rates between $\dot{\epsilon} = 1$ and 10 s $^{-1}$, whereas at lower $\dot{\epsilon}$ the SHF rapidly decays to one. Interestingly, whereas for the pom-pom the SHF further increases with increasing strain rate, the SHF of

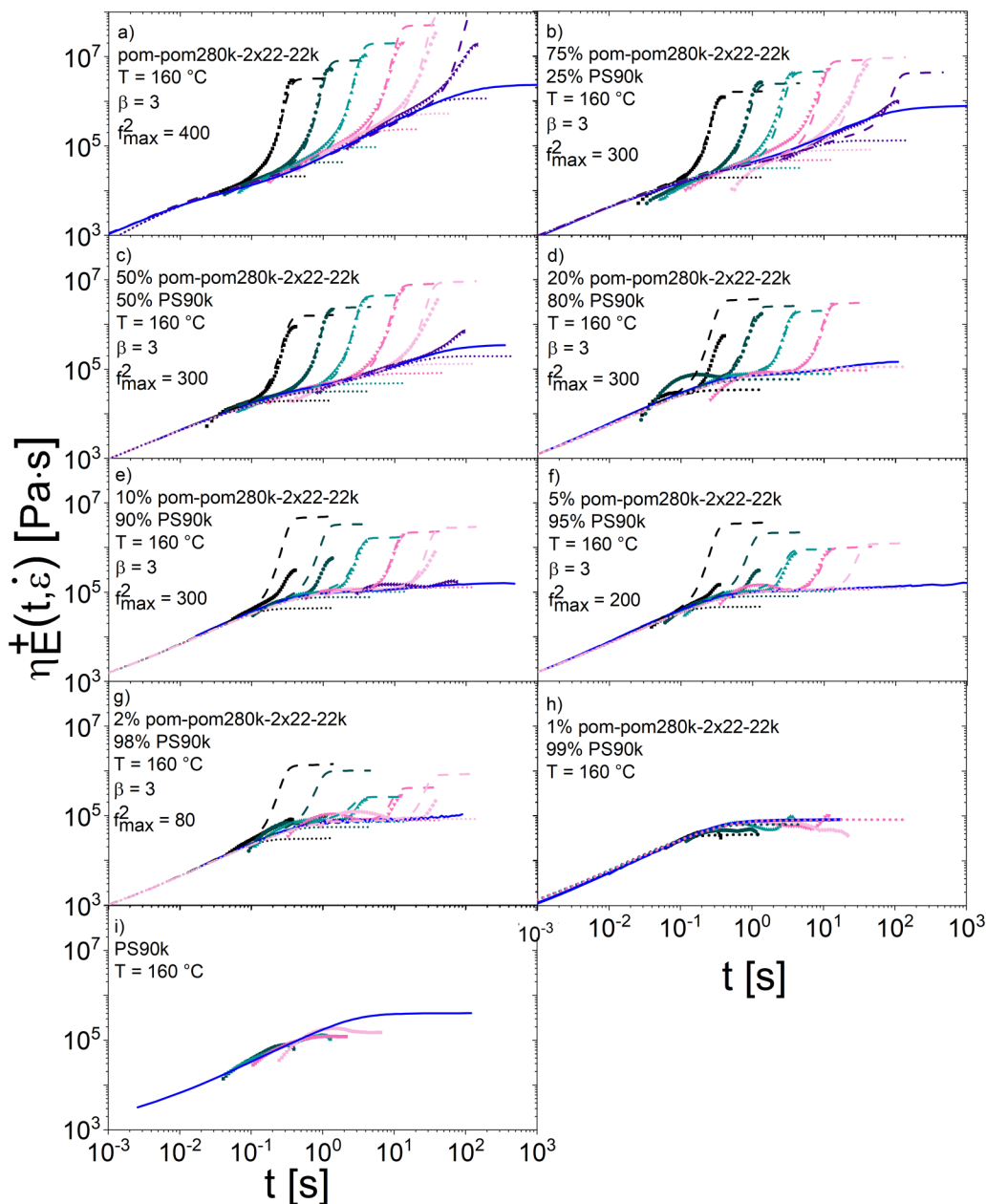


FIG. 8. The tensile stress growth coefficient as a function of the step time for pom-pom280k-2x22-22k and the blends of linear PS90k with the pom-pom for $\phi_{\text{pom-pom}} = 100, 75, 50, 20, 10, 5, 2, 1,$ and 0 wt. % pom-pom at a temperature of $T = 160$ °C. The legend for the Hencky strain rates, the LVE envelope, and the DE and MSF models is the same as for Fig. 7.

the blends decreases again at high strain rates. To compare the maximum SHF, SHF_{max} is plotted in Fig. 10(c) as a function of the pom-pom content, revealing that for PS43k blends with $\phi_{\text{pom-pom}} = 75$ wt. % and $\phi_{\text{pom-pom}} = 50$ wt. % the maximum SHFs are $\text{SHF}_{\text{max}} = 105$ and $\text{SHF}_{\text{max}} = 121$, respectively, which are within the experimental error margin quasisimilar than for the pure pom-pom. The blend with only $\phi_{\text{pom-pom}} = 20$ wt. % still provides SHF up to $\text{SHF}_{\text{max}} = 65$, whereas for $\phi_{\text{pom-pom}} = 10$ wt. % $\text{SHF}_{\text{max}} = 33$ and for $\phi_{\text{pom-pom}} = 5$ wt. % the maximum SHF is still $\text{SHF}_{\text{max}} = 15$. A $\text{SHF}_{\text{max}} = 10$ can be reached for $\phi_{\text{pom-pom}} = 2$ wt. % at $\dot{\epsilon} = 10$ s $^{-1}$, where even $\phi_{\text{pom-pom}} = 1$ wt. % results in $\text{SHF} = 4$.

As seen from Fig. 10(b), the blends with PS90k show the highest SHF between 0.1 and 1 s $^{-1}$, and the blends with $\phi_{\text{pom-pom}} = 75$ and 50 wt. % can only reach a similar

SHF as the pure pom-pom at lower strain rates of 0.3 and 0.1 s $^{-1}$, respectively. As presented in Figs. 10(b) and 10(c), $\phi_{\text{pom-pom}} = 75$ wt. % and $\phi_{\text{pom-pom}} = 50$ wt. % in PS90k result in maximum SHF around $\text{SHF}_{\text{max}} = 90$, $\phi_{\text{pom-pom}} = 20$ wt. % in $\text{SHF}_{\text{max}} = 33$, $\phi_{\text{pom-pom}} = 10$ wt. % in $\text{SHF}_{\text{max}} = 15$, $\phi_{\text{pom-pom}} = 5$ wt. % in $\text{SHF}_{\text{max}} = 8$ and for only $\phi_{\text{pom-pom}} = 2$ wt. % low strain hardening around $\text{SHF} = 4$ remains, whereas only little strain hardening of $\text{SHF}_{\text{max}} = 1.5$ can be observed for $\phi_{\text{pom-pom}} = 1$ wt. %. Again, up to $\phi_{\text{pom-pom}} = 50$ wt. % with linear PS, SHF_{max} depends only little on the linear PS content. This is a very interesting finding as it allows to uncouple zero-shear viscosity and elongational properties very nicely.

Comparing the maximum SHF as a function of the Hencky strain rate, the PS90k blends reveal the highest SHFs

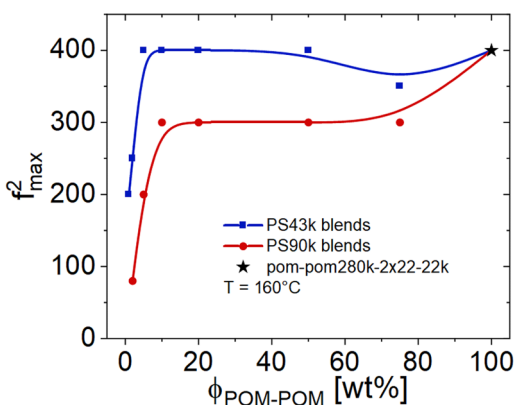


FIG. 9. The parameter f_{\max}^2 of the MSF model as a function of the pom-pom weight content for the blends with PS43k and PS90k. The f_{\max}^2 trends show clearly that above 5–10 wt. % pom-pom one f_{\max}^2 value can be used to model the data successfully.

in a medium $\dot{\epsilon}$ range between $\dot{\epsilon} = 0.1$ and 1 s^{-1} , whereas for the PS43k blends the SHF_{\max} can typically be observed at larger strain rates between $\dot{\epsilon} = 1$ and 10 s^{-1} . So, compared with the pure pom-pom, for the blends with $\phi_{\text{pom-pom}} = 50 \text{ wt. \%}$ lower SHFs are reached at high $\dot{\epsilon}$, but at $\dot{\epsilon} = 1 \text{ s}^{-1}$ (PS43k) and $\dot{\epsilon} = 0.3 \text{ s}^{-1}$ (PS90k) identical SHF as the pom-pom of about $\text{SHF} = 120$ and 90 are reached.

The high SHF for high linear PS content is astonishing, considering that commercial LDPE and PP have SHF typically around 10 [21,60,67,68]. To set it in perspective, a blend with only $\phi_{\text{pom-pom}} = 2 \text{ wt. \%}$ in linear PS43k gave a

$\text{SHF} = 10$ and for PS90k $\text{SHF} = 4$. This underlines the importance of topology to tailor processing additives and that a thorough understanding of the impact of topology is key. In comparison, LDPE, which is often added as a processing additive to LLDPE, is an ill-defined branched system with a mainly comb-like structure, and it seems to be significantly less effective as a strain hardening agent. Additionally, the strain hardening at very low pom-pom contents might confirm that traces of LCB might be the cause of strain hardening in some HDPE grades, as evidently very low amounts are sufficient to still create some strain hardening [69].

To further investigate the strain hardening and the effect of lower zero-shear viscosity due to dilution with linear chains, in Fig. 11(a) the maximum value of the tensile stress growth coefficient, $\eta_{E,\max}^+$, and in (b) and (c) $\eta_{E,\max}^+$ normalized to $3\eta_0$, are plotted as a function of the Weissenberg number, $Wi = \tau_1 \dot{\epsilon}$, where τ_1 is the longest relaxation time in the blend [57]. The measurements are limited to Hencky strains of $\epsilon = 4$, so the elongational viscosity is not (always) reached. However, the curves flatten and do not indicate (significantly) higher $\eta_{E,\max}^+$. For the pure pom-pom, $\eta_{E,\max}^+$ has a maximum at $Wi = 57$, followed by a decrease with a slope of about -0.5 , i.e., $\eta_{E,\max}^+ \propto Wi^{-0.5}$. In general, the pom-pom blends with both, PS43k and PS90k, have their $\eta_{E,\max}^+$ maximum around the same Wi number. The maximum tensile stress growth coefficient is larger for the PS90k blends than for the PS43k blends and with decreasing pom-pom content, this effect is more pronounced. Only for 75 wt. % pom-pom at $Wi > 100$, both blends with the same

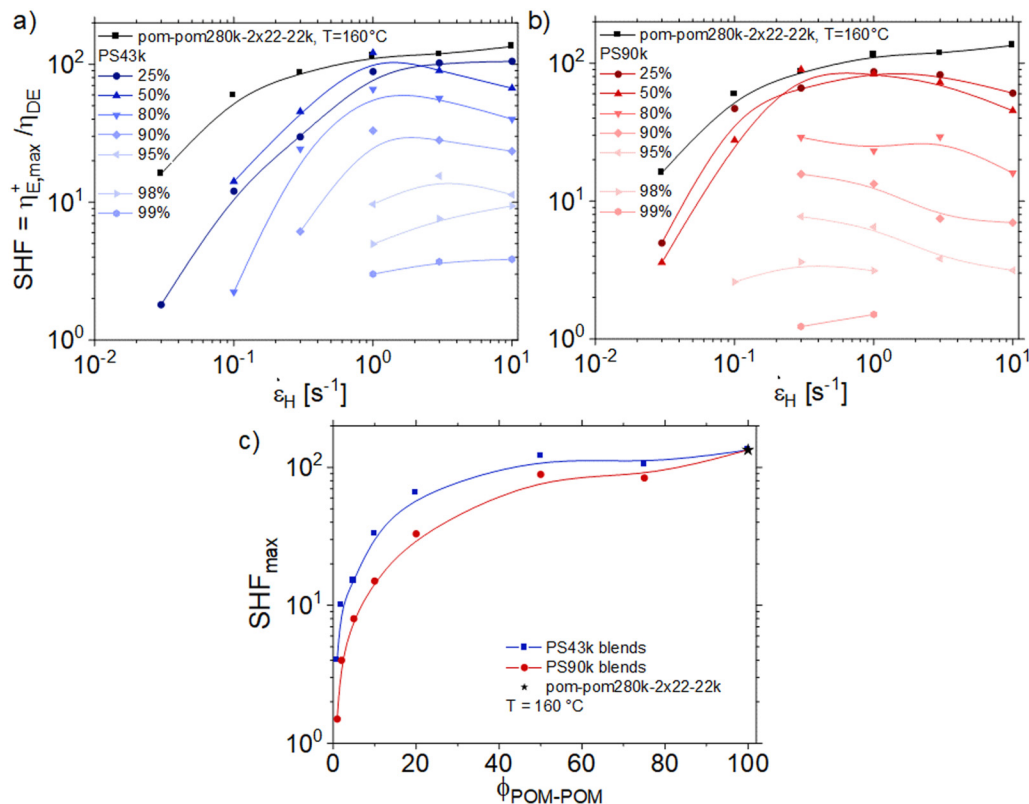


FIG. 10. SHFs as a function of the Hencky strain rate for the blends of the pom-pom with (a) the PS43k and (b) the PS90k and in (c) the maximum SHF as a function of the pom-pom content for blends with both polymers.

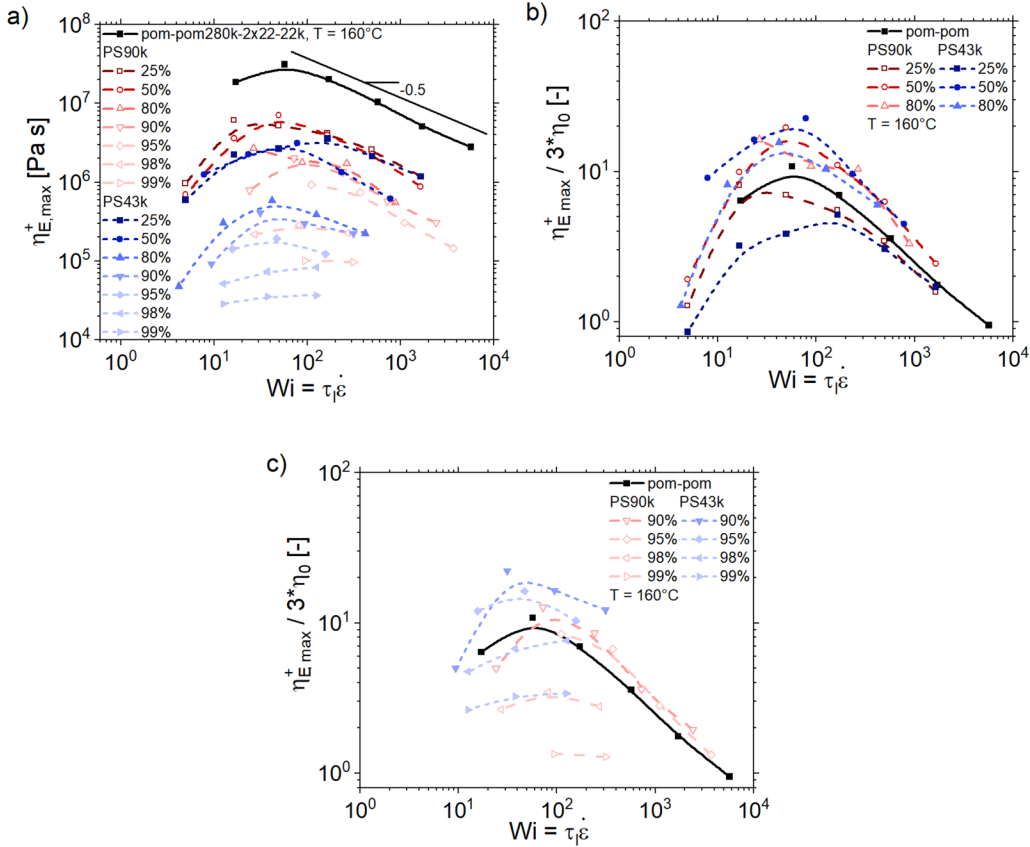


FIG. 11. (a) Maximum value of the tensile stress growth coefficient and [(b) and (c)] the maximum value of the tensile stress growth coefficient normalized to $3\eta_0$, as a function of the Weissenberg number ($Wi = \tau_0 \dot{\epsilon}$) for the pure pom-pom (square) and the blends of PS43k and PS90k. The full line indicates a slope of -0.5 .

pom-pom content have similar $\eta_{E,max}^+$. At lower pom-pom contents, the difference is up to one decade.

Similar to the pure pom-pom, also for the blends a similar scaling of $\eta_{E,max}^+ \propto Wi^{-0.5}$ can be found at $Wi > 57$, matching the observations found for linear mono- and bi-disperse blends, as well as Cayley-tree polymers [35,70,71].

Figures 11(b) and 11(c) combine η_0 in Fig. 3 with $\eta_{E,max}^+$ from Fig. 11(a) as $\eta_{E,max}^+ / 3\eta_0$. First, for blends containing 20, 50, and 75 wt. % pom-pom, the values of $\eta_{E,max}^+ / 3\eta_0$ (mainly) overlap for the PS43k and PS90k blends, i.e., the relative strain hardening caused by topology is independent of the linear matrix. For lower pom-pom contents, this is not true anymore and the values of the blends with PS43k are lower than with PS90k.

Furthermore, $\eta_{E,max}^+ / 3\eta_0$ at similar Wi is lower in the 75 wt. % blend than in the 50 wt. % blend for both linear PS. This explains why the blends with $\phi_{\text{pom-pom}} = 50$ wt. % have higher SHF_{max} than for $\phi_{\text{pom-pom}} = 75$ wt. %, as shown in Fig. 11. For both pom-pom weight fractions, $\eta_{E,max}^+ / 3\eta_0$ is significantly lower in the 75 wt. % blends than in the 50 wt. % blends, since $\eta_{E,max}^+$ are in a similar range at equal $\dot{\epsilon}$. However, the linear viscoelastic response decreases with decreasing pom-pom content, so also the SHF at $\phi_{\text{pom-pom}} = 50$ wt. % becomes larger than at $\phi_{\text{pom-pom}} = 75$ wt. %.

Consequently, it can be investigated if the dilution effect from the linear PS chains on the pom-pom is more pronounced on the shear or the elongational behavior. For

example, the pure pom-pom and the 50 wt. % PS43k blend differ in η_0 by a factor of about 20, but at the highest strain rate measured of $\dot{\epsilon} = 10 \text{ s}^{-1}$, $\eta_{E,max}^+$ decreases only by a factor around 2.5. Comparing the blends of PS43k and PS90k, i.e., η_0 differs more than $\eta_{E,max}^+$. For example, at 50 wt. % pom-pom, η_0 differs for the PS43k and PS90k blends by a factor of 2.7, but $\eta_{E,max}^+$ at 10 s^{-1} only by a factor of 1.4. Consequently, the dilution effect from the linear PS chains on the pom-pom is more pronounced in shear than in elongation.

In the literature, four blends of two linear PS with 10 wt. % PS820k ($M_w = 820 \text{ kg mol}^{-1}$) and 90% $M_w = 9, 23, 34,$ and 73 kg mol^{-1} components were investigated at 130°C in uniaxial elongation. At the measurement conditions of similar Wi , $\eta_{E,max}^+$ was found to be independent of the M_w of the low M_w component [57]. For strain hardening induced by the pom-pom topology at $T = 160^\circ\text{C}$ in a blend, this is evidently not the case, as $\eta_{E,max}^+$ decreases with decreasing molecular weight of the linear PS, but rather $\eta_{E,max}^+ / 3\eta_0$ overlaps at similar Wi for the different linear PS for, e.g., 50 wt. % pom-pom.

The results presented here show that the relationship between strain hardening behavior under elongational deformation and zero-shear viscosity in shear can be uncoupled by blending of linear and pom-pom shaped polymers. Comparing blends with similar η_0 but highly different SHFs underlines this effect. For example, $\phi_{\text{pom-pom}} = 50$ wt. % in

PS43k and $\phi_{\text{pom-pom}} = 5$ wt. % in PS90k have the same η_0 , but totally different maximum SHF of $\text{SHF}_{\text{max}} = 120$ and 9, respectively. Furthermore, combining the semilogarithmic zero-shear viscosity dependency on the pom-pom content in Fig. 3(c) and the MSF model parameters in Fig. 9 allows us to simply predict the elongational behavior and strain hardening of linear/pom-pom blends at strain rates below the inverse of the Rouse time of the linear polymer and to minimize experimental work.

V. CONCLUSION

Blending of polymers allows one to tune rheological properties and has a huge industrial importance in the processing of, e.g., polyethylene and PP, where linear grades are blended with branched ones. Nevertheless, blends of linear with well-defined branched model systems were rarely investigated in the past. In this work, the shear and elongational rheology of blends of two linear PS with $M_w = 43$ and 90 kg mol^{-1} and a pom-pom shaped PS ($M_{w,bb} = 280 \text{ kg mol}^{-1}$, $M_{w,a} = 22 \text{ kg mol}^{-1}$, $q = 22$) was investigated experimentally. Additionally, the experimental data were modeled using constitutive models such as the DE model and the MSF model. Under small amplitude oscillatory shear, the results show a semilogarithmic relationship between pom-pom weight content and the zero-shear viscosity. Whereas the pure pom-pom has in uniaxial elongational flow SHFs of more than $\text{SHF} = 100$, similar values can be found for blends with up to $\phi_{\text{pom-pom}} = 50$ wt. %. By blending only $\phi_{\text{pom-pom}} = 2$ wt. % with linear PS43k, a $\text{SHF} = 10$ can still be measured. The results show that the relationship between melt and elongational behavior, i.e., between zero-shear viscosity and SHF, can be uncoupled by the blending of linear and pom-pom shaped polymers.

Furthermore, above $\phi_{\text{pom-pom}} = 5$ and 10 wt. %, respectively, the extensional behavior can be well-described with the MSF with a single parameter set of $\beta = 3$ and $f_{\text{max}}^2 = 400$ for PS43k and $f_{\text{max}}^2 = 300$ for PS90k. Combined with the semilogarithmic η_0 dependency on the pom-pom weight fraction described above, the shear and elongational behavior of those blends can be well predicted.

Moreover, this work raises the question, if pom-pom shaped polymers are highly suitable candidates as additives in recycling as well as for biopolymers with little melt strength to ensure good processability.

ACKNOWLEDGMENTS

The authors acknowledge Professor H. Henning Winter and the IRIS software team for access to their IRIS Rheo-Hub software. Furthermore, the authors thank Marie-Christine Röpert for proofreading the manuscript as well as Michael Pollard for proofreading the manuscript as a native English speaker. The authors would like to thank Professor Manfred Wilhelm for all the support in general, especially the access to the great infrastructure and working environment available, as well as for highly fruitful discussions. Finally, we would like to thank the anonymous reviewers for their critiques and comments, which helped to further improve the manuscript.

AUTHOR DECLARATIONS

Conflict of Interest

The authors have no conflicts to disclose.

REFERENCES

- [1] Dealy, J. M., *Structure and Rheology of Molten Polymers: From Polymerization to Processability Via Rheology: From Structure to Flow Behavior and Back Again* (Hanser Gardner Publications, Munich, 2006).
- [2] Macosko, C. W., *Rheology Principles, Measurements and Applications*, edited by C. W. Macosko (Wiley-VCH, Chichester, 1994).
- [3] Hyun, K., and M. Wilhelm, "Establishing a new mechanical nonlinear coefficient q from FT-rheology: First investigation of entangled linear and comb polymer model systems," *Macromolecules* **42**, 411–422 (2009).
- [4] Cziep, M. A., M. Abbasi, M. Heck, L. Arens, and M. Wilhelm, "Effect of molecular weight, polydispersity, and monomer of linear homopolymer melts on the intrinsic mechanical nonlinearity $3Q_0(\omega)$ in MAOS," *Macromolecules* **49**, 3566–3579 (2016).
- [5] Fang, Y., P. J. Carreau, and P. G. Lafleur, "Thermal and rheological properties of mLLDPE/LDPE blends," *Polym. Eng. Sci.* **45**(9), 1254–1264 (2005).
- [6] Aji, A., P. Sammut, and M. A. Huneault, "Elongational rheology of LLDPE/LDPE blends," *J. Appl. Polym. Sci.* **88**, 3070–3077 (2003).
- [7] Ahirwal, D., S. Filipe, I. Neuhaus, M. Busch, G. Schlatter, and M. Wilhelm, "Large amplitude oscillatory shear and uniaxial extensional rheology of blends from linear and long-chain branched polyethylene and polypropylene," *J. Rheol.* **58**, 635–658 (2014).
- [8] Wagner, M. H., S. Kheirandish, J. Stange, and H. Münstedt, "Modeling elongational viscosity of blends of linear and long-chain branched polypropylenes," *Rheol. Acta* **46**, 211–221 (2006).
- [9] Maroufkhani, M., and N. Golshan Ebrahimi, "Melt rheology of linear and long-chain branched polypropylene blends," *Iran. Polym. J.* **24**, 715–724 (2015).
- [10] Stange, J., C. Uhl, and H. Münstedt, "Rheological behavior of blends from a linear and a long-chain branched polypropylene," *J. Rheol.* **49**, 1059–1079 (2005).
- [11] Nouri, S., C. Dubois, and P. G. Lafleur, "Effect of chemical and physical branching on rheological behavior of polylactide," *J. Rheol.* **59**, 1045–1063 (2015).
- [12] Hassan, M. M., T. Takahashi, and K. Koyama, "Thermal stability, mechanical properties, impact strength, and uniaxial extensional rheology of reactive blends of PS and SBS polymers," *Polym. Bull.* **76**, 5537–5557 (2019).
- [13] López-Barrón, C. R., Y. Zeng, and J. J. Richards, "Chain stretching and recoiling during startup and cessation of extensional flow of bidisperse polystyrene blends," *J. Rheol.* **61**, 697–710 (2017).
- [14] Wagner, M. H., V. H. Rolón-Garrido, J. K. Nielsen, H. K. Rasmussen, and O. Hassager, "A constitutive analysis of transient and steady-state elongational viscosities of bidisperse polystyrene blends," *J. Rheol.* **52**, 67–86 (2008).
- [15] Nielsen, J. K., H. K. Rasmussen, O. Hassager, and G. McKinley, "Elongational viscosity of monodisperse and bidisperse polystyrene melts," *J. Rheol.* **50**, 453–476 (2006).
- [16] Ianniruberto, G., G. Marrucci, and Y. Masubuchi, "Melts of linear polymers in fast flows," *Macromolecules* **53**, 5023–5033 (2020).
- [17] Zhou, Y., C. D. Young, M. Lee, S. Banik, D. Kong, G. B. McKenna, R. M. Robertson-Anderson, C. E. Sing, and C. M. Schroeder, "Dynamics and rheology of ring-linear blend semidilute solutions in

- extensional flow: Single molecule experiments," *J. Rheol.* **65**, 729–744 (2021).
- [18] Borger, A., W. Wang, T. C. O'Connor, T. Ge, G. S. Grest, G. V. Jensen, J. Ahn, T. Chang, O. Hassager, K. Mortensen, D. Vlassopoulos, and Q. Huang, "Threading–unthreading transition of linear-ring polymer blends in extensional flow," *ACS Macro Lett.* **9**, 1452–1457 (2020).
- [19] Wagner, M. H., E. Narimissa, and T. Shahid, "Elongational viscosity and brittle fracture of bidisperse blends of a high and several low molar mass polystyrenes," *Rheol. Acta* **60**, 803–817 (2021).
- [20] Abbasi, M., L. Faust, K. Riazzi, and M. Wilhelm, "Linear and extensional rheology of model branched polystyrenes: From loosely grafted combs to bottlebrushes," *Macromolecules* **50**, 5964–5977 (2017).
- [21] Münstedt, H., "Extensional rheology and processing of polymeric materials," *Int. Polym. Process.* **33**(3532), 594–618 (2018).
- [22] Huang, Q., "When polymer chains are highly aligned: A perspective on extensional rheology," *Macromolecules* **55**, 715–727 (2022).
- [23] Lentzakis, H., D. Vlassopoulos, D. J. Read, H. Lee, T. Chang, P. Driva, and N. Hadjichristidis, "Uniaxial extensional rheology of well-characterized comb polymers," *J. Rheol.* **57**, 605–625 (2013).
- [24] López-Barrón, C. R., M. E. Shivokhin, and J. R. Hagadorn, "Extensional rheology of highly-entangled α -olefin molecular bottlebrushes," *J. Rheol.* **63**, 917–926 (2019).
- [25] Tan, L., J. Pan, and A. Wan, "Shear and extensional rheology of polyacrylonitrile solution: Effect of ultrahigh molecular weight polyacrylonitrile," *Colloid Polym. Sci.* **290**, 289–295 (2012).
- [26] Szántó, L., Y. Feng, and C. Friedrich, "Extensional hardening of multimodal, linear PE with high amounts of UHMWPE," *J. Rheol.* **65**, 371–380 (2021).
- [27] Wagner, M. H., S. Kheirandish, K. Koyama, A. Nishioka, A. Minegishi, and T. Takahashi, "Modeling strain hardening of polydisperse polystyrene melts by molecular stress function theory," *Rheol. Acta* **44**, 235–243 (2005).
- [28] Wingstrand, S. L., M. van Drongelen, K. Mortensen, R. S. Graham, Q. Huang, and O. Hassager, "Influence of extensional stress overshoot on crystallization of LDPE," *Macromolecules* **50**, 1134–1140 (2017).
- [29] McLeish, T. C. B., and R. G. Larson, "Molecular constitutive equations for a class of branched polymers: The pom-pom polymer," *J. Rheol.* **42**, 81–110 (1998).
- [30] McLeish, T. C. B., J. Allgaier, D. K. Bick, G. Bishko, P. Biswas, R. Blackwell, B. Blottière, N. Clarke, B. Gibbs, D. J. Groves, A. Hakiki, R. K. Heenan, J. M. Johnson, R. Kant, D. J. Read, and R. N. Young, "Dynamics of entangled H-polymers: Theory, rheology, and neutron-scattering," *Macromolecules* **32**, 6734–6758 (1999).
- [31] Inkson, N. J., T. C. B. McLeish, O. G. Harlen, and D. J. Groves, "Predicting low density polyethylene melt rheology in elongational and shear flows with 'pom-pom' constitutive equations," *J. Rheol.* **43**, 873–896 (1999).
- [32] Kempf, M., D. Ahirwal, M. Cziep, and M. Wilhelm, "Synthesis and linear and nonlinear melt rheology of well-defined comb architectures of PS and PpMS with a low and controlled degree of long-chain branching," *Macromolecules* **46**, 4978–4994 (2013).
- [33] Abbasi, M., L. Faust, and M. Wilhelm, "Comb and bottlebrush polymers with superior rheological and mechanical properties," *Adv. Mater.* **31**, 1806484 (2019).
- [34] Röpert, M.-C., M. G. Schußmann, M. K. Esfahani, M. Wilhelm, and V. Hirschberg, "Effect of side chain length in polystyrene POM–POMs on melt rheology and solid mechanical fatigue," *Macromolecules* **55**, 5485–5496 (2022).
- [35] van Ruymbeke, E., E. B. Muliawan, S. G. Hatzikiriakos, T. Watanabe, A. Hirao, and D. Vlassopoulos, "Viscoelasticity and extensional rheology of model Cayley-tree polymers of different generations," *J. Rheol.* **54**, 643–662 (2010).
- [36] McLeish, T. C. B., "Tube theory of entangled polymer dynamics," *Adv. Phys.* **51**, 1379–1527 (2002).
- [37] Wagner, M. H., S. Kheirandish, and M. Yamaguchi, "Quantitative analysis of melt elongational behavior of LLDPE/LDPE blends," *Rheol. Acta* **44**, 198–218 (2004).
- [38] Doi, M., and S. F. Edwards, *The Theory of Polymer Dynamics* (Clarendon, Oxford, 2013), Vol. 73.
- [39] de Gennes, P. G., "Reptation of a polymer chain in the presence of fixed obstacles," *J. Chem. Phys.* **55**, 572–579 (1971).
- [40] Rubinstein, M., and R. H. Colby, *Polymer Physics* (Oxford University, Oxford, 2014).
- [41] Wagner, M. H., P. Ehrecke, P. Hachmann, and J. Meissner, "A constitutive analysis of uniaxial, equibiaxial and planar extension of a commercial linear high-density polyethylene melt," *J. Rheol.* **42**, 621–638 (1998).
- [42] Rolón-Garrido, V. H., R. Pivokonsky, P. Filip, M. Zatloukal, and M. H. Wagner, "Modelling elongational and shear rheology of two LDPE melts," *Rheol. Acta* **48**, 691–697 (2009).
- [43] Rolón-Garrido, V. H., "The molecular stress function (MSF) model in rheology," *Rheol. Acta* **53**, 663–700 (2014).
- [44] Wagner, M. H., M. Yamaguchi, and M. Takahashi, "Quantitative assessment of strain hardening of low-density polyethylene melts by the molecular stress function model," *J. Rheol.* **47**, 779–793 (2003).
- [45] Wagner, M. H., P. Rubio, and H. Bastian, "The molecular stress function model for polydisperse polymer melts with dissipative convective constraint release," *J. Rheol.* **45**, 1387–1412 (2001).
- [46] Kheirandish, S., and M. Stadlbauer, "Molecular stress function theory and analysis of branching structure in industrial polyolefins," *J. Therm. Anal. Calorim.* **98**, 629–637 (2009).
- [47] Houli, S., H. Iatrou, N. Hadjichristidis, and D. Vlassopoulos, "Synthesis and viscoelastic properties of model dumbbell copolymers consisting of a polystyrene connector and two 32-arm star polybutadienes," *Macromolecules* **35**, 6592–6597 (2002).
- [48] Polymeropoulos, G., G. Zapsas, K. Ntetsikas, P. Bilalis, Y. Gnanou, and N. Hadjichristidis, "50th anniversary perspective: Polymers with complex architectures," *Macromolecules* **50**, 1253–1290 (2017).
- [49] Nielsen, J. K., H. K. Rasmussen, M. Denberg, K. Almdal, and O. Hassager, "Nonlinear branch-point dynamics of multiarm polystyrene," *Macromolecules* **39**, 8844–8853 (2006).
- [50] Faust, L., M.-C. Röpert, M. K. Esfahani, M. Abbasi, V. Hirschberg, and M. Wilhelm, "Comb and branch-on-branch model polystyrenes with exceptionally high strain hardening factor SHF > 1000 and their impact on physical foaming," *Macromol. Chem. Phys.* **224**, 2200214 (2023).
- [51] Röpert, M.-C., A. Goecke, M. Wilhelm, and V. Hirschberg, "Threading polystyrene stars: Impact of star to POM-POM and barbwire topology on melt rheological and foaming properties," *Macromol. Chem. Phys.* **223**, 2200288 (2022).
- [52] Hadjichristidis, N., M. Pitsikalis, S. Pispas, and H. Iatrou, "Polymers with complex architecture by living anionic polymerization," *Chem. Rev.* **101**, 3747–3792 (2001).
- [53] Hadjichristidis, N., H. Iatrou, M. Pitsikalis, and J. Mays, "Macromolecular architectures by living and controlled/living polymerizations," *Prog. Polym. Sci.* **31**, 1068–1132 (2006).
- [54] Zhang, H., J. Zhu, J. He, F. Qiu, H. Zhang, Y. Yang, H. Lee, and T. Chang, "Easy synthesis of dendrimer-like polymers through a divergent iterative 'end-grafting' method," *Polym. Chem.* **4**, 830–839 (2013).
- [55] Yuan, Z., and M. Gauthier, "Synthesis of arborescent isoprene homopolymers," *Macromolecules* **38**, 4124–4132 (2005).

- [56] Moingeon, F., Y. R. Wu, L. E. Cadena-Sánchez, and M. Gauthier, "Synthesis of arborescent styrene homopolymers and copolymers from epoxidized substrates," *J. Polym. Sci., Part A: Polym. Chem.* **50**, 1819–1826 (2012).
- [57] Shahid, T., C. Clasen, F. Oosterlinck, and E. van Ruymbeke, "Diluting entangled polymers affects transient hardening but not their steady elongational viscosity," *Macromolecules* **52**, 2521–2530 (2019).
- [58] Poh, L., E. Narimissa, M. H. Wagner, and H. H. Winter, "Interactive shear and extensional rheology—25 years of IRIS software," *Rheol. Acta* **61**, 259–269 (2022).
- [59] Winter, H. H., and M. Mours, "The cyber infrastructure initiative for rheology," *Rheol. Acta* **45**, 331–338 (2006).
- [60] Zhang, H., T. Liu, B. Li, H. Li, Z. Cao, G. Jin, L. Zhao, and Z. Xin, "Evaluating melt foamability of LLDPE/LDPE blends with high LLDPE content by bubble coalescence mechanism," *Polymer* **213**, 123209 (2021).
- [61] Ianniello, V., and S. Costanzo, "Linear and nonlinear shear rheology of nearly unentangled H-polymer melts and solutions," *Rheol. Acta* **61**, 667–679 (2022).
- [62] Liu, C., J. Wang, and J. He, "Rheological and thermal properties of m-LLDPE blends with m-HDPE and LDPE," *Polymer* **43**, 3811–3818 (2002).
- [63] Ebrahimi, T., H. Taghipour, D. Griebel, P. Mehrkhodavandi, S. G. Hatzikiriakos, and E. van Ruymbeke, "Binary blends of entangled star and linear poly(hydroxybutyrate): Effect of constraint release and dynamic tube dilation," *Macromolecules* **50**, 2535–2546 (2017).
- [64] Lentzakis, H., S. Costanzo, D. Vlassopoulos, R. H. Colby, D. J. Read, H. Lee, T. Chang, and E. van Ruymbeke, "Constraint release mechanisms for H-polymers moving in linear matrices of varying molar masses," *Macromolecules* **52**, 3010–3028 (2019).
- [65] Wagner, M. H., E. Narimissa, L. Poh, and Q. Huang, "Modelling elongational viscosity overshoot and brittle fracture of low-density polyethylene melts," *Rheol. Acta* **61**, 281–298 (2022).
- [66] Rasmussen, H. K., J. K. Nielsen, A. Bach, and O. Hassager, "Viscosity overshoot in the start-up of uniaxial elongation of low density polyethylene melts," *J. Rheol.* **49**, 369–381 (2005).
- [67] Huang, Q., M. Mangnus, N. J. Alvarez, R. Koopmans, and O. Hassager, "A new look at extensional rheology of low-density polyethylene," *Rheol. Acta* **55**, 343–350 (2016).
- [68] Gabriel, C., and H. Münstedt, "Strain hardening of various polyolefins in uniaxial elongational flow," *J. Rheol.* **47**, 619–630 (2003).
- [69] Morelly, S. L., and N. J. Alvarez, "Characterizing long-chain branching in commercial HDPE samples via linear viscoelasticity and extensional rheology," *Rheol. Acta* **59**, 797–807 (2020).
- [70] Marrucci, G., and G. Ianniruberto, "Interchain pressure effect in extensional flows of entangled polymer melts," *Macromolecules* **37**, 3934–3942 (2004).
- [71] Matsumiya, Y., and H. Watanabe, "Non-universal features in uniaxially extensional rheology of linear polymer melts and concentrated solutions: A review," *Prog. Polym. Sci.* **112**, 101325 (2021).
- [72] See supplementary material at <https://www.scitation.org/doi/suppl/10.1122/8.0000544> for the complete mastercurves of the blends.